European Radiology (2019) 29:2792–2801
https://doi.org/10.1007/s00330-018-5879-z

MAGNETIC RESONANCE

Magnetic resonance spectroscopy in posterior fossa tumours: the tumour spectroscopic signature may improve discrimination in adults among haemangioblastoma, ependymal tumours, medulloblastoma, and metastasis

Paloma Mora[1] · Albert Pons[2] · Mónica Cos[2] · Angels Camins[2] · Amadeo Muntané[1] · Carles Aguilera[2,3] · Carles Arús[3,4,5] · Carles Majós[2,3]

Received: 17 July 2018 / Revised: 8 October 2018 / Accepted: 8 November 2018 / Published online: 19 December 2018

Abstract

Objectives Assessing a posterior fossa tumour in an adult can be challenging. Metastasis, haemangioblastoma, ependymal tumours, and medulloblastoma are the most common diagnostic possibilities. Our aim was to evaluate the contribution of magnetic resonance spectroscopy (MRS) in the diagnosis of these entities.

Methods We retrospectively evaluated 56 consecutive patients with a posterior fossa tumour and histological diagnosis of ependymal tumour, medulloblastoma, haemangioblastoma, and metastasis in which good-quality spectra at short (TE 30 ms) or/and intermediate (TE, 136 ms) TE were available. Spectra were compared using the Mann-Whitney *U* non-parametric test in order to select the spectral datapoints and the intensity ratios that showed significant differences between groups of lesions. Performance of these datapoints and their ratios were assessed with ROC curves.

Results The most characteristic signatures on spectroscopy were high choline (Cho) in medulloblastoma ($p < 0.001$), high myoinositol (mIns) in ependymal tumours ($p < 0.05$), and high lipids (LIP) in haemangioblastoma ($p < 0.01$) and metastasis ($p < 0.01$). Selected ratios between normalised intensity signals of resonances provided accuracy values between 79 and 95% for pairwise comparisons. Intensity ratio $NI_{3.21ppm/3.55ppm}$ provided satisfactory discrimination between medulloblastoma and ependymal tumours (accuracy, 92%), ratio $NI_{2.11ppm/1.10ppm}$ discriminated ependymal tumours from haemangioblastoma (accuracy, 94%), ratio $NI_{3.21ppm/1.13ppm}$ discriminated haemangioblastoma from medulloblastoma (accuracy, 95%), and ratio $NI_{1.28ppm/2.02pmm}$ discriminated haemangioblastoma from metastasis (accuracy, 83%).

Conclusions MRS may improve the non-invasive diagnosis of posterior fossa tumours in adults.

Key Points

- *High choline suggests a medulloblastoma in a posterior fossa tumour.*
- *High myoinositol suggests an ependymal lesion in a posterior fossa tumour.*
- *High lipids suggest a metastasis or a haemangioblastoma in a posterior fossa tumour.*

Keywords Magnetic resonance imaging · Magnetic resonance spectroscopy · Posterior fossa tumours · Neoplasm metastasis

✉ Paloma Mora
palomamora@bellvitgehospital.cat; pombamora@gmail.com

[1] Department of Radiology, Hospital Universitari de Bellvitge, L'Hospitalet de Llobregat, Spain

[2] Department of Radiology, Institut de Diagnòstic per la Imatge (IDI), Centre Bellvitge, Hospital Universitari de Bellvitge, L'Hospitalet de Llobregat, Spain

[3] Centro de Investigación Biomédica en Red en Bioingeniería, Biomateriales y Nanomedicina (CIBER-BBN), Cerdanyola del Vallès, Spain

[4] Departament de Bioquímica i Biologia Molecular, Unitat de Bioquímica de Biociències, Edifici Cs, Universitat Autònoma de Barcelona, Cerdanyola del Vallès, Spain

[5] Institut de Biotecnologia i de Biomedicina (IBB), Universitat Autònoma de Barcelona, Cerdanyola del Vallès, Spain

Abbreviation

Cho	Choline
Glx	Glutamine-glutamate
LIP	Lipids
MRS	Magnetic resonance spectroscopy
mIns	Myoinositol
NI	Normalised to unit length datapoint intensities

Introduction

Assessing a posterior fossa tumour represents a challenge for the radiologist. A fast response must be given not only to raise diagnostic suspicion but also to avoid complications derived from a troublesome location. In this context, the role of the radiologist in the multidisciplinary management of the patient is highly relevant. Posterior fossa tumours are infrequent lesions in adults [1]. Metastasis, haemangioblastoma, ependymal tumours, and medulloblastoma are the most common possibilities [2]. Discrimination among these entities has relevant implications in patient management. Thus, localising the primary tumour and performing a precise staging are mandatory when a solitary metastasis is suspected [3]. Ependymal lesions and medulloblastoma are tumours with a tendency to CSF dissemination [4], and a whole spine exam must be performed before planning further treatment. Moreover, haemangioblastoma is a slow-growing tumour in which delayed treatment may even be suggested depending on the clinical situation of the patient [5, 6].

Several previous studies have assessed MRS findings of common brain tumours [7–9]. Posterior fossa common malignancies have been reviewed in the pediatric population [10–17]. Nevertheless, there is little in the literature about spectroscopic findings of posterior fossa tumours in adults [18].

The aim of this study was to evaluate the contribution of magnetic resonance spectroscopy (MRS) in the diagnosis of posterior fossa tumours in adults. We focused our attention on the signatures of each particular tumour that might allow to confident differentiation between them.

Methods

Patients

We retrospectively evaluated 74 consecutive patients with a posterior fossa tumour and histological diagnosis of ependymoma/subependymoma, medulloblastoma, haemangioblastoma, or metastasis in whom spectroscopy was performed between June 1997 and December 2017. All tumours had a definitive histological diagnosis and were untreated. All metastases were solitary posterior fossa lesions. This retrospective study was included in a research project that had local ethics committee approval. Unspecific informed consent to participate in research projects was obtained from all patients. Waiver of a specific informed consent was provided by the Ethics Committee for this retrospective study.

MRI and MRS

MRI and single-voxel MRS were performed on a 1.5-T MR imaging unit (Philips Healthcare). Single-voxel MRS was incorporated in the standard imaging study. The VOI was between 1.5 cm × 1.5 cm × 1.5 cm (3.4 cc) and 2 cm × 2 cm × 2 cm (8 cc). It was placed so as to position the largest possible voxel within the solid tumour seen on MRI. The homogeneity of the magnetic field in the VOI was optimised automatically. Two spectra were obtained with a water-suppressed, single-voxel, point-resolved spectroscopic sequence (PRESS) from the same VOI: 1) short TE (TR/TE/averages, 2000/30/96–192) and intermediate TE (2000/136/128–256). The standard receiver head coil was used in all cases. The quality of the spectra was evaluated by visual inspection. The visual analysis was performed by two neuroradiologists blinded to patient data with 22 and 9 years of experience in MRS (CM and PM). A spectrum was considered to be of poor quality when large peak linewidth (water linewidth > 8 Hz), poor signal intensity-to-noise ratio (SNR < 10), or obvious artifacts (high scalp lipids, poor phasing, large baseline artifacts, or metabolite peaks of suspected origin evaluated by expert spectroscopist) precluded precise evaluation of some regions of the spectrum.

Poor-quality spectra were excluded from the study; these corresponded to three spectra at short TE (two medulloblastoma and one metastasis) and nine spectra at both TE (two medulloblastoma, three haemangioblastoma, and four metastases).

Spectrum analysis was performed off-line with the use of the jMRUI software [19]. All spectra were processed by CM and PM. The signal intensities of data points in the spectrum between 0 and 4.00 ppm (total, 130 data points) were selected and used as input for the normalisation and statistical analysis. Each datapoint intensity in the spectrum was normalised to the unit ($NI_{x.xxppm}$) [20]. Chemical shifts in the frequency domain were internally referenced to Cr 3.03 ppm and/or Cho 3.21 ppm. Average spectra were constructed for each tumour type and TE with the normalised spectra. Several ratios between the intensity signals of the points ($NI_{x.xxppm/x.xxppm}$) were calculated.

Statistics

Spectra were evaluated as a series of numbers drawing the graphic shown as spectra. Each point in the spectrum was considered a variable for the statistical analysis. Lesions were compared using the Mann-Whitney *U* non-parametric test. The test was used to assess differences between pairs of tumours types. Then we constructed some concrete ratios based on the performance of the points with significant differences. Because multiple variables were considered for every test, we corrected the obtained *p* values

using the Hochberg method (p^*) [21]. Only datapoints with significance level better than $p^* < 0.05$ were considered relevant resonances to differentiate each tumour type. To improve the consistency of the results, we used only those points having two neighboring points with significant differences. ROC curves were constructed to identify the points that provided the best relationship between sensitivity and specificity. Those points were used as cut-off points for the classifiers. Values of sensitivity, specificity, and accuracy were calculated to provide an estimate of the expected performance when applied in clinical practice.

All statistical computations were performed using SPSS 14.0 software (SPSS Inc.).

Results

Patients

We retrieved from our archives 6 ependymoma, 4 subependymoma, 22 medulloblastoma, 12 haemangioblastoma, and 30 metastasis cases. Ependymoma and subependymoma are uncommon tumours in adulthood and have been reported to show similar findings [22]. These tumours were combined in our study into a single group, namely "ependymal tumours," to perform bilateral comparisons with other groups. In 9 patients, the spectroscopic raw data could not be retrieved and analysed (one subependymoma, one haemangioblastoma, three medulloblastomas, and four metastases). These patients were excluded from the study. A qualitative assessment of the spectra was performed in the remaining 65 patients and poor-quality spectra were also excluded (9 cases at both TE and 3 more cases at short TE only). The final dataset included 56 patients (ependymal tumours, 9 patients; medulloblastoma, 17 patients; haemangioblastoma, 8 patients; solitary metastasis, 22 patients). Demographic characteristics of patients finally included in the dataset are shown in Table 1.

Spectroscopic signatures

Mean spectra for each tumour type are shown in Fig. 1. Visual analysis of mean spectra at short and intermediate TE showed particular signatures for each tumour type. Large resonances of mIns at $NI_{3.55ppm}$ at short TE were found in ependymal tumours. Low resonances at $NI_{3.55ppm}$ were found in metastasis and haemangioblastoma, and intermediate values were found in medulloblastoma. Medulloblastoma was characterised by large resonances of Cho at $NI_{3.22ppm}$ at short TE. This signature remained, although less prominent, at intermediate TE. Metastasis was characterised by the presence of broad resonances centred at $NI_{1.25ppm}$ at intermediate TE. Haemangioblastoma showed intermediate amounts of LIP, with a narrow resonance at $NI_{2.02ppm}$.

Tumour classification

Bilateral comparisons between pairs of tumour types were made to orientate the differential diagnosis. These comparisons worked better at short TE for all bilateral comparison procedures, except for the comparison between metastasis and haemangioblastoma. A high resonance centred at $NI_{3.21ppm}$ was the most prominent finding of medulloblastoma in pairwise comparisons, showing significant differences with all tumour types ($p^* < .001$ with haemangioblastoma and metastasis at both TE; $p^* < .001$ at short TE and $p^* < .01$ at intermediate TE with ependymal tumours). Broad resonances in the $NI_{1.25ppm}$ region were a characteristic finding of metastasis, with significant differences with medulloblastoma ($p^* < .001$), ependymal tumours ($p^* < .001$), and haemangioblastoma ($p^* < .01$) at short TE. Ependymal tumours showed some differences in the $NI_{3.55ppm}$ at short TE with all tumour types ($p^* < .01$ with metastasis and $p^* < .05$ with medulloblastoma and haemangioblastoma). Additional differences between tumour types can be found in Table 2 as well as the level of significance in each case (p^*). These characteristics may be further observed in Figs. 2, 3, 4, and 5.

Classifiers were constructed on the basis of these findings. We constructed ratios between the resonances that we felt might provide better discrimination between tumour types. The suggested ratios, jointly with the cut-off points for classification and the accuracy obtained in our dataset, are shown in Table 3. The ratio Cho/mIns discriminated medulloblastoma from ependymal tumours with satisfactory accuracy ($NI_{3.21ppm}$/

Table 1 Patient demographics

Tumour type	Original dataset	Final dataset					
	Subjects	Subjects	Short TE	Intermediate TE	Females	Mean age (range)	Mean size (range
Ependymal tumours*	10	9	9	9	6	45 (25–48)	35.8 (43.5–19.4)
Medulloblastoma	22	17	15	17	6	30 (17–44)	39.3 (52.7–24.9)
Haemangioblastoma	12	8	8	8	5	58 (38–67)	35.3 (47–28.6)
Metastasis	30	22	21	22	7	60 (45–82)	32.3 (48–20.3)

*"Ependymal tumours" group includes ependymoma and subependymoma histology

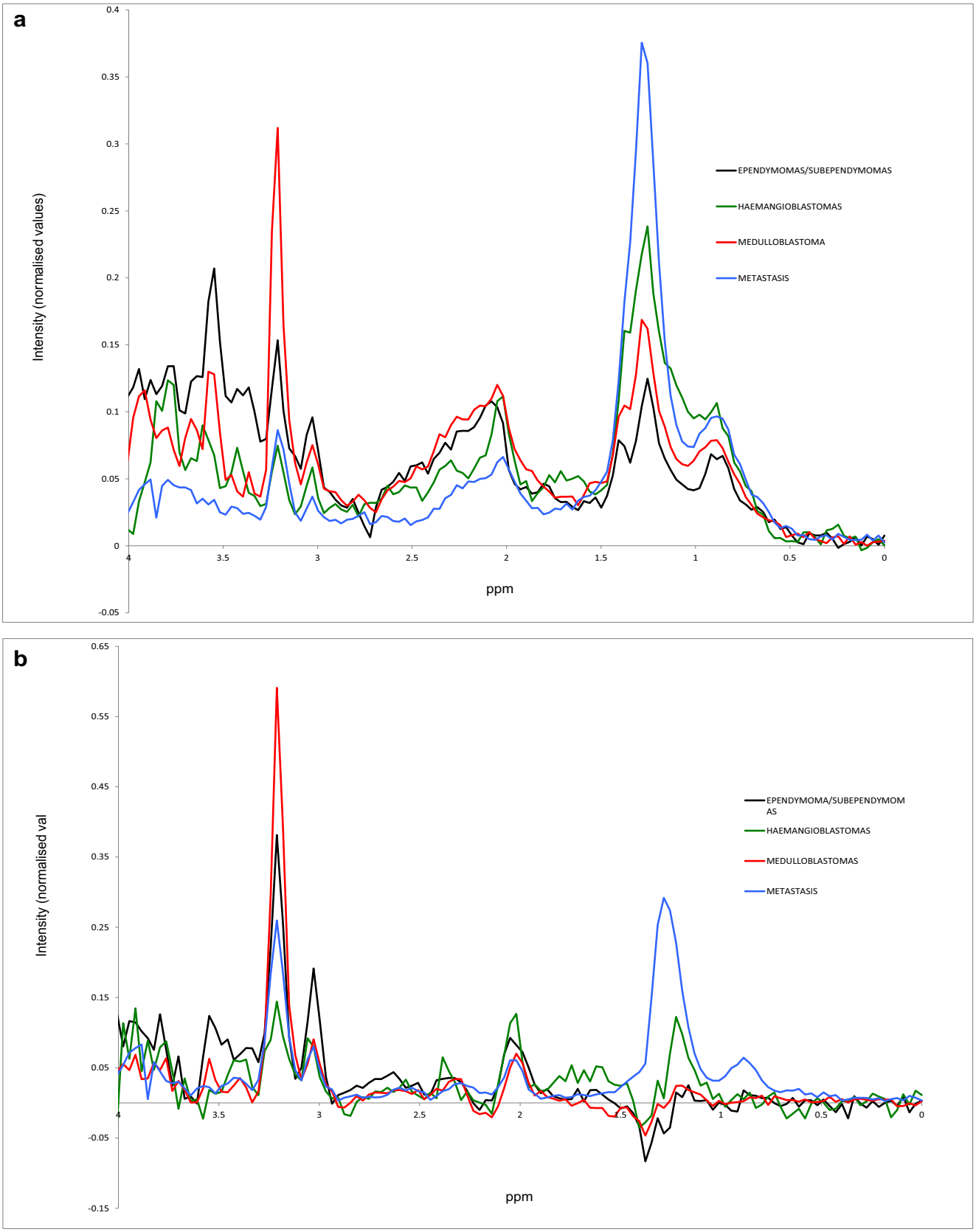

Fig. 1 Average spectra of ependymal lesions, medulloblastoma, haemangioblastoma, and metastasis calculated with all the cases included in the study for short TE (**a**) and intermediate TE (**b**)

Table 2 Results of Mann-Whitney *U* non-parametric test comparisons

	$p^* < .05$	$p^* < .01$	$p^* < .001$
Medulloblastoma vs. ependymal tumours			
Short TE	3.55	3.79	3.21
			3.43
Intermediate TE		2.05	3.49
		3.21	
		3.03	
Medulloblastoma vs. haemangioblastoma			
Short TE		1.13	3.21
		2.11	
Intermediate TE		3.55	3.21
Medulloblastoma vs. metastasis			
Short TE	0.9	3.03	1.25, 1.28
	3.46	3.36	2.05, 2, 11, 3.55
			3.21
Intermediate TE			0.92, 1.25, 1.28
			2.14
			3.21
Ependymal tumours vs. haemangioblastoma			
Short TE	3.55	2.11	1.10
		3.30	
Intermediate TE		3.21	
		3.46	
		3.55	
Ependymal tumours vs. metastasis			
Short TE	0.9	3.55	1.25, 1.28
	2.02		2.11, 3.03, 3.36
	3.21		3.43, 3.79
Intermediate TE		3.49	0.98, 1.25, 1.28
			3.03
			3.55
Metastasis vs. haemangioblastoma			
Short TE		1.25	
		1.28	
Intermediate TE	0.9		

NI resonances with statistically significant differences between tumour groups shown in short and intermediate TE

*Differences of *p* corrected values < .05 were considered to be statistically significant

$_{3.55ppm}$; accuracy, 92% at both TE). Medulloblastoma could be satisfactorily discriminated from metastasis on the basis of the Cho/LIP ratio ($NI_{3.21ppm/1.28ppm}$; accuracy, 89% at short TE and 82% at intermediate TE). The ratio between Cho and LIP also allowed good discrimination between medulloblastoma and haemangioblastoma (short TE, $NI_{3.21ppm/1.13ppm}$; accuracy, 95%; intermediate TE, $NI_{3.21\ ppm/1.22ppm}$; accuracy, 87%). The ratio Glx/LIP discriminated ependymal tumours from haemangioblastoma with satisfactory accuracy (short TE, $NI_{2.11ppm/1.10ppm}$; accuracy, 94%). Ependymal tumours were satisfactorily discriminated from metastasis on the basis of the LIP/mIns ratio ($NI_{1.28ppm/3.55ppm}$; accuracy, 90% at both TE). The ratio between LIP and *N*-acetyl-containing compounds allowed good discrimination between metastasis and haemangioblastoma (short TE, $NI_{1.28ppm/2.02ppm}$; accuracy, 79%; intermediate TE, $NI_{1.28\ ppm/2.02ppm}$; accuracy, 83%).

Discussion

The most common tumours in the posterior fossa in adulthood include metastasis, haemangioblastoma, ependymal tumours, and medulloblastoma [1]. The gold standard for the diagnosis of these tumours remains histological analysis. Nevertheless, clinical management is largely influenced by the suspected pre-surgical diagnosis.

MRI findings may provide a first diagnostic approach in posterior fossa tumours. Haemangioblastoma usually corresponds to a cystic lesion located in the cerebellar vermis with a solid mural enhancing nodule. Nevertheless, in 40% of cases, it appears as a solid lesion without any cystic component, and in 85% of cases, it can be located in the cerebellar hemisphere [23]. In adults, medulloblastomas usually are located in cerebellar hemispheres [18], and cyst formation or necrosis degeneration is frequent [24]. In 10–20% of cases, they show intralesional calcifications [24, 25]. Ependymoma can also be found as heterogeneous intraparenchymal lesions with solid or cystic components, calcifications, and hemorrhage, or as predominantly cystic lesions with a mural nodule [26]. On the basis of these imaging features, the differential diagnosis between haemangioblastoma, medulloblastoma, and ependymal tumours can be challenging. What's more, metastases are the most common diagnosis in this location in middle-aged and older patients [1] and their imaging appearance could overlap with primary posterior fossa tumours.

MRS has been proven to be useful in diagnosing the most common brain tumours [7–9]. Less prevalent tumours, such as posterior fossa tumours in adults, have received little attention, and the clinical application of spectroscopy in these cases has not been assessed in depth. MRS provides biochemical information through the resonances or individual data points in the spectrum that can be correlated with the contribution of particular metabolites. In children, medulloblastoma has been suggested as showing increased taurine with high Cho and low NAA [11–17], while ependymoma has been described as displaying high mIns levels at short TE, in association with high Cho and low NAA [10, 13, 14]. Meanwhile, there is little information about the spectroscopic signatures of haemangioblastoma [27].

A possible approach to the application of spectroscopy in a clinically real situation is by defining some signatures that could be considered as "biochemical markers" of the tumours. In our study, medulloblastomas showed very high levels of

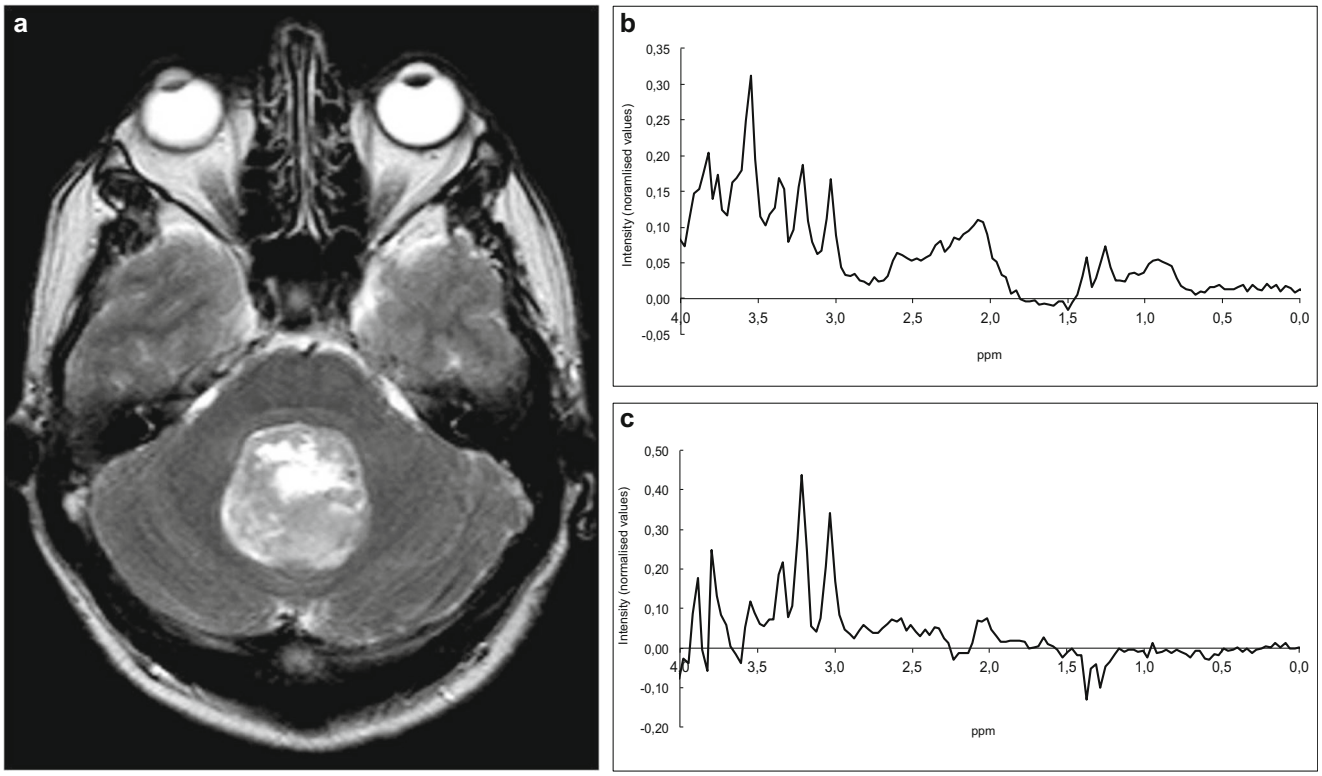

Fig. 2 Subependymoma. **a** T2WI shows a hyperintense lesion on the posterior aspect of the pontine mesencephalic junction. **b** MRS at short TE shows high mIns and low LIP. **c** MRS at intermediate TE shows low Cho/Cr ratio

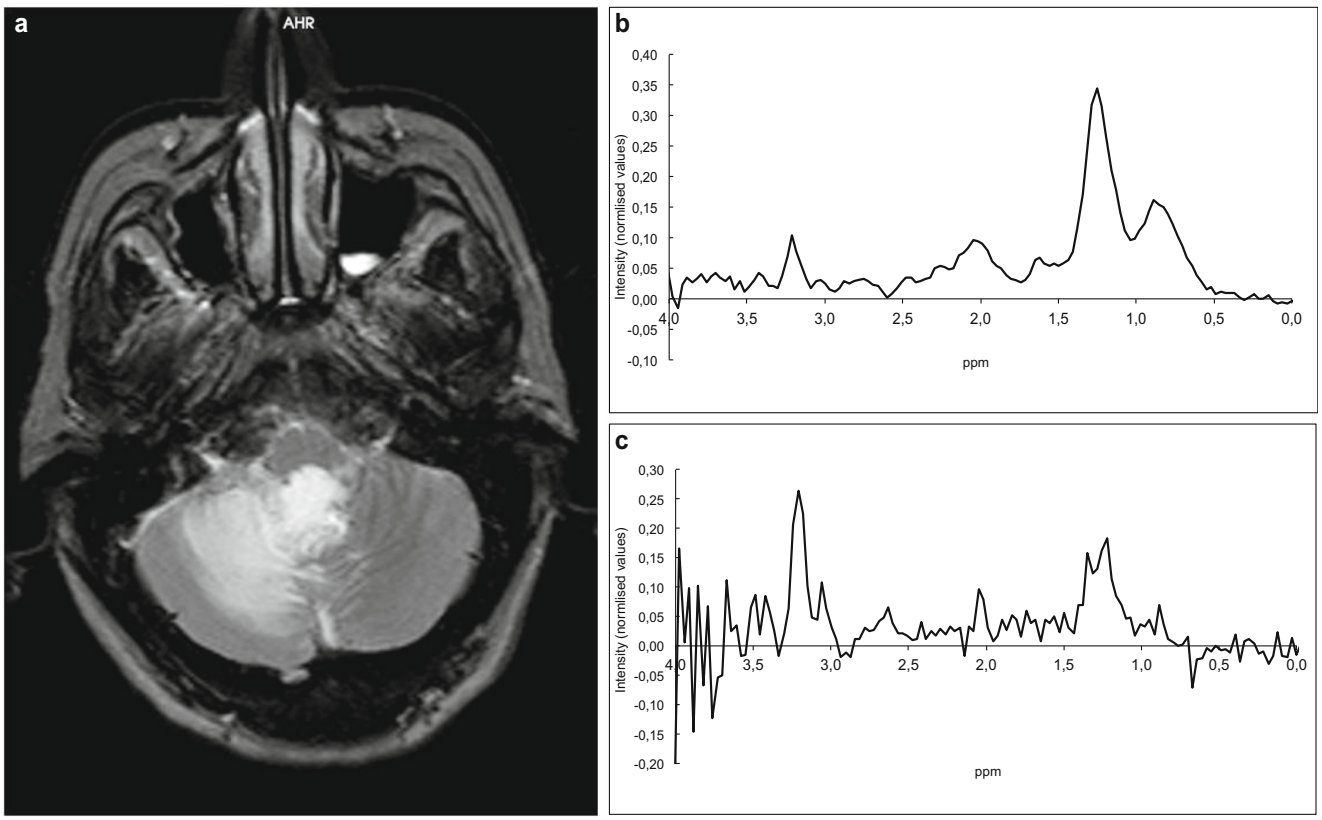

Fig. 3 Haemangioblastoma. **a** T2WI shows a hyperintense pontine lesion. **b** MRS at short TE shows high LIP and low $NI_{2.11}$ and Cho. **c** 1H-MR spectroscopy at intermediate TE shows relatively low Cho compared with medulloblastoma and ependymal tumours

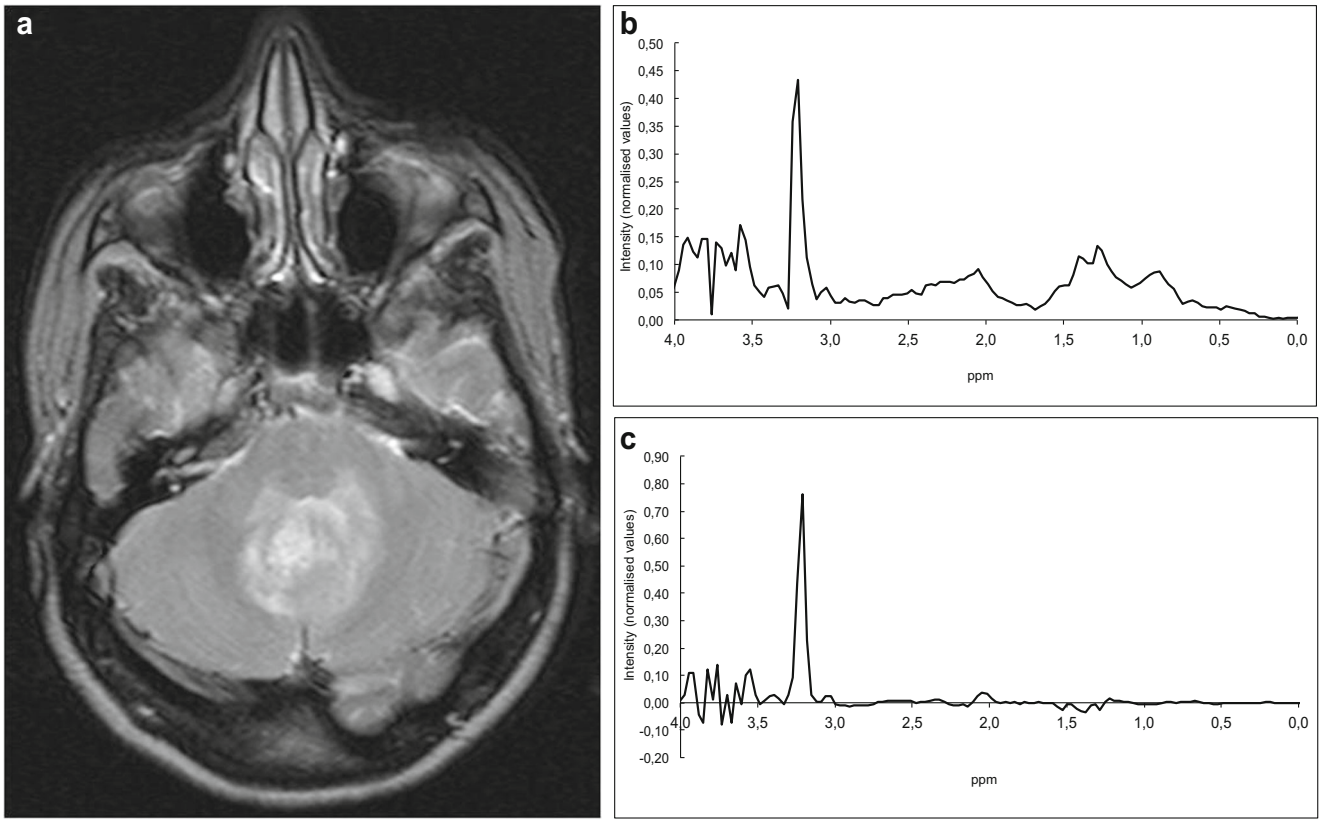

Fig. 4 Medulloblastoma. **a** T2WI shows a hyperintense lesion in the posterior aspect of the fourth ventricle. **b** MRS at short TE shows very high Cho and low $NI_{3.43}$. **c** MRS at intermediate TE also shows very high Cho

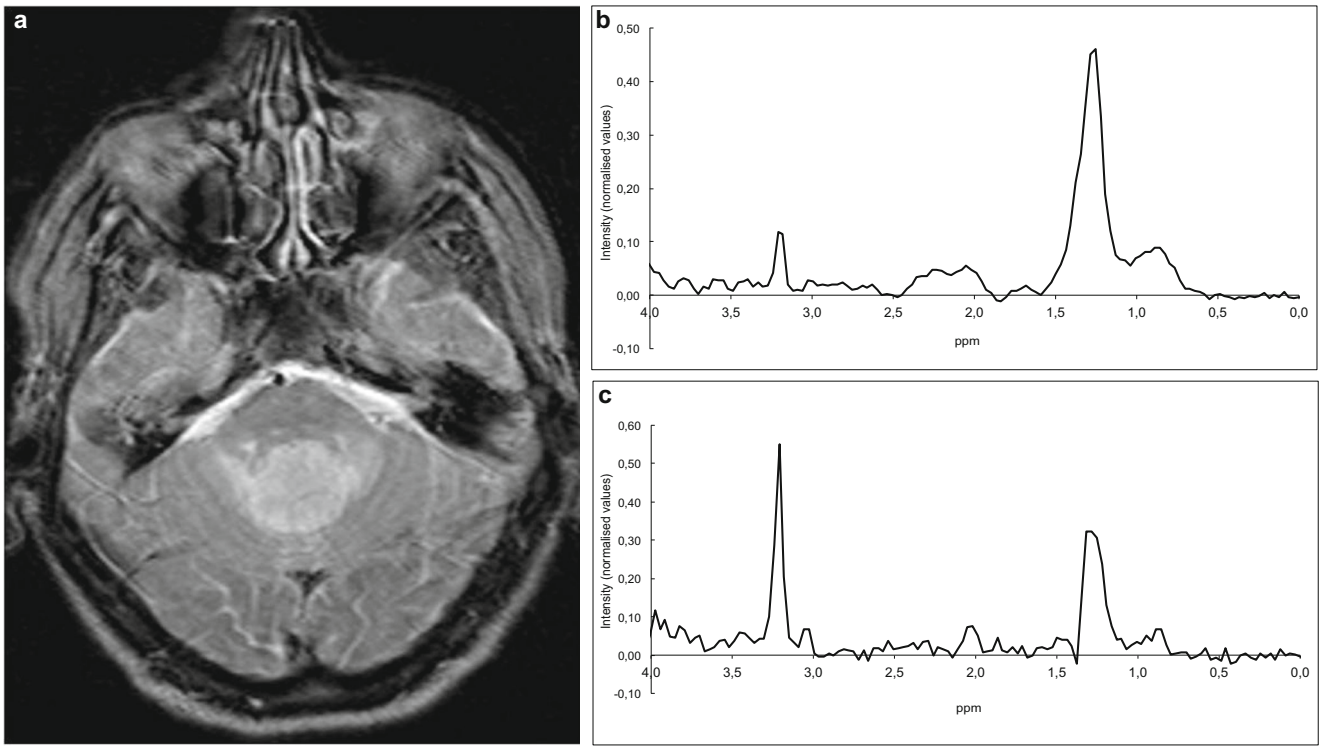

Fig. 5 Metastasis. **a** T2WI shows a hyperintense lesion of the pontine mesencephalic junction. **b** MRS at short TE shows high LIP and some Cho. **c** MRS at intermediate TE also shows high LIP-lactate and high Cho. Please note great similarity between T2WI in Figs. 2, 3, 4, and 5 with some spectroscopic differential signatures in panels **b** and **c** that could orientate in the differential diagnosis

Table 3 Accuracy values obtained using ROC curves for the selected ratios

	$NI_{x.xx/NIx.xx}$[1]	AUC[2]	Cut-off point[3]	Accuracy (%)
Medulloblastoma vs ependymal lesions				
Short TE	3.21/3.55	0.926	0.82	92
Intermediate TE	3.21/3.55	0.837	4.18	92
Medulloblastoma vs haemangioblastoma				
Short TE	3.21/1.13	0.971	0.63	95
Intermediate TE	3.21/1.22	0.748	2.82	87
Medulloblastoma vs metastasis				
Short TE	3.22/1.28	0.952	0.39	89
Intermediate TE	3.22/1.28	0.695	3.19	82
Ependymal lesions vs haemangioblastoma				
Short TE	2.11/1.10	0.984	1.32	94
Intermediate TE	3.21/1.22	0.714	4.40	81
Ependymal lesions vs metastasis				
Short TE	1.28/3.55	0.894	2.72	90
Intermediate TE	1.28/3.55	0.864	1.31	90
Metastasis vs haemangioblastoma				
Short TE	1.28/2.02	0.714	3.49	79
Intermediate TE	1.28/2.02	0.656	1.88	83

[1] NIx.xx/NIx.xx: ratio between intensity signals of points

[2] Area under the curve

[3] Cut-off points of normalised intensity (NI) values on ROC curves

choline-containing compound at $NI_{3.22ppm}$. Cho is a salient component of the Kennedy pathway involved in the genesis of phospholipid of the cell membrane. The presence of choline peaks in MRS spectra reflects increased cell membrane synthesis and thus increased cellularity [28]. An increased Cho has been found in several kinds of tumours, including meningioma, astrocytoma, and lymphoma. The levels that we have found in medulloblastoma seem even higher than those found in other kinds of tumours. This finding was previously reported by Majós et al [18] and may be related to high cellular density.

Myoinositol is a sugar. According to the results in our study, it could be considered a biochemical marker on ependymal tumours. It is believed to be an osmolyte involved in osmoregulation and volume regulation that has been found increased in other gliomas too [29]. Increased levels of mlns are believed to reflect increased numbers of glial cells. Nevertheless, the levels of mIns that we have found in ependymal tumours are significantly higher than those reported in the literature in astrocytomas and in oligodendrogliomas [30]. The significance of these high levels of mIns is unknown and should be explored in further work. Ependymal tumours and medulloblastoma also showed resonances at $NI_{2.02ppm}$, corresponding to broad resonances between $NI_{2.00\ and\ 2.50ppm}$, partially inverted at intermediate TE, attributable to Glx [31].

We have found that intermediate values of LIP jointly with a narrow resonance of *N*-acetyl-containing compounds at $NI_{2.02ppm}$ are the most relevant characteristic of haemangioblastoma. On the other hand, very high values of mobile LIP centred at $NI_{1.25ppm}$ were the most relevant signature of metastasis. Lipids have been related to necrosis and have been mainly found in metastasis and glioblastoma. The lipid peaks detected in most of these processes are predominantly saturated lipids believed to arise from increased number of cytoplasmic vesicles, especially in tissues demonstrating necrosis and inflammation [29]. Nevertheless, we have found that it may be employed to satisfactorily differentiate the spectroscopic pattern of haemangioblastomas and metastasis to those of ependymal lesions and medulloblastomas.

Based on our results, some resonances in the spectrum may be used as markers for particular tumour histologies in posterior fossa tumours. High Cho at $NI_{3.22ppm}$ may be considered a signature of medulloblastoma, mainly at short TE, high mIns at $NI_{3.55ppm}$ at short TE is characteristic of ependymal tumours, and high mobile LIP centred at $NI_{1.25ppm}$ is characteristic of metastasis. Haemangioblastoma does not show a prominent marker in our study, but is suggested when intermediate values of LIPs are found jointly with a narrow resonance of *N*-acetyl-containing compounds at $NI_{2.02ppm}$. These visual and statistical differences may be quantitatively applied with satisfactory accuracy by means of ratios among Cho, mIns, LIP, and NAA and may be used to discriminate among these posterior fossa lesions.

Several limitations can be seen in our study. First, there is the low number of tumours evaluated in each group. This is the reason why we could not discriminate between histological subtypes of medulloblastoma and the reason why we combined ependymoma and subependymoma into a single group. There is an inherent limitation of uncommon tumours that precludes a more precise pre-surgical characterisation by spectroscopy. Another limitation related to the low number of cases is that we could not save a cohort of patients to be used as an independent test set cohort. We felt that reducing the number of cases used to construct the classifier would have produced a worse classifier. The present absence of a subgroup of patients to be used as a test cohort may affect the reproducibility of the results of our work. A larger multicentre study could partially solve the limitation, but including cases acquired with different MR equipment and software may require still larger numbers of patients to reduce the effects of instrumental variability in the recorded data. Another limiting condition is that large susceptibility artifacts may affect spectroscopy in the posterior fossa; however, they can be reduced by carefully selecting the voxel position and by excluding low-quality spectra from analysis. This should be taken into account because the application of our findings to low-quality spectra could produce results not supported by our work.

In summary, we believe that MRS may play a role in the non-invasive assessment of posterior fossa tumours in adults by limiting the differential diagnosis and improving the clinical management of these patients. We found that medulloblastoma displays high Cho at short and intermediate TE, ependymal lesions share high mIns values at short TE, metastasis presents high LIP resonances, and haemangioblastoma shows intermediate LIP with a narrow resonance of *N*-acetyl-containing compounds, as their most relevant metabolic signatures.

Funding This work was partially funded by the Ministerio de Economía y Competitividad (MINECO) grant MOLIMAGLIO (SAF2014-52332-R). It was also funded by Centro de Investigación Biomédica en Red – Bioingeniería, Biomateriales y Nanomedicina (CIBER-BBN, [http://www.ciber-bbn.es/en]), an initiative of the Instituto de Salud Carlos III (Spain) co-funded by EU Fondo Europeo de Desarrollo Regional (FEDER).

Compliance with ethical standards

Guarantor The scientific guarantor of this publication is Carlos Majós MD, PhD.

Conflict of interest The authors of this manuscript declare no relationships with any companies, whose products or services may be related to the subject matter of the article.

Statistics and biometry One of the authors has significant statistical expertise.

Informed consent Written informed consent was obtained from all subjects (patients) in this study.

Ethical approval Institutional Review Board approval was obtained.

Study subjects or cohorts overlap Some study subjects or cohorts have been previously reported in:

a. Majós C, Alonso J, Aguilera C, et al (2003) Proton magnetic resonance spectroscopy (1H MRS) of human brain tumours: assessment of differences between tumour types and its applicability in brain tumour categorization. Eur Radio 13:582–91.

b. Mora P, Majós C, Castañer S, et al (2014) ^{1}H-MRS is useful to reinforce the suspicion of primary central nervous system lymphoma prior to surgery. Eur Radiol 24:2895–905.

c. Majós C, Alonso J, Aguilera C, Serrallonga M, Acebes JJ, Arús C, Gili J. Adult primitive neuroectodermal tumour: Proton MR Spectroscopic findings with possible application for differential diagnosis. Radiology 2002;225:556–566.

d. Majós C, Julià-Sapé M, Alonso J, Serrallonga M, Aguilera C, Acebes JJ, Arús C, Gili J. Brain tumor classification by proton MR spectroscopy: comparison of diagnostic accuracy at short and long TE. AJNR *Am J Neuroradiol* 2004;25:1696–1704.

e. Majós C, Aguilera C, Cos M, Camins A, Candiota AP, Delgado-Goñi T, Samitier A, Castañer S, Sánchez JJ, Mato D, Acebes JJ, Arús C. In vivo proton magnetic resonance spectroscopy of intraventricular tumours of the Brain. Eur Radiol 2009;19:2049–2059.

Methodology

- retrospective
- diagnostic or prognostic study/observational
- performed at one institution

References

1. Ostrom QT, Gittleman H, Liao P et al (2014) CBTRUS statistical report: primary brain and central nervous system tumors diagnosed in the United States in 2007-2011. Neuro Oncol 16:iv1–iv63
2. Grossman R, Ram Z (2016) Posterior fossa intra-axial tumors in adults. World Neurosurgery 88:140–145
3. Eichler AF, Loeffler JS (2007) Multidisciplinary management of brain metastasis. Oncologist 12:884–898
4. North C, Segall HD, Stanley P, Zee CS, Ahmadi J, McComb JG (1985) Early detection on intracranial seeding from medulloblastoma. AJNR Am J Neuroradiol 6:11–13
5. Kanno H, Kobayashi N, Nakanowatari S (2014) Pathological and clinical features and management of central nervous system hemangioblastomas in von Hippel-Lindau disease. J Kidney Cancer VHL 1:46–55
6. Slater A, Moore NR, Huson SM (2003) The natural history of cerebellar hemangioblastomas in von Hippel-Lindau disease. AJNR Am J Neuroradiol 24:1570–1574
7. Dowling C, Bollen AW, Noworolski SM et al (2001) Preoperative proton MR spectroscopy imaging of brain tumors: correlation with histopathologic analysis of resection specimens. AJNR Am J Neuroradiol 22:604–612
8. Howe FA, Barton SJ, Cudlip SA et al (2003) Metabolic profiles of human brain tumors using quantitative in vivo ^{1}H magnetic resonance spectroscopy. Magn Reson Med 49:223–232
9. Majós C, Julià-Sapé M, Alonso J et al (2004) Brain tumor classification by proton MR spectroscopy: comparison of diagnostic accuracy at short and long TE. AJNR Am J Neuroradiol 25:1696–1704
10. Harris LM, Davies N, Macpherson L et al (2007) The use of short TE 1H MRS for childhood cerebellar tumours prior to histopathological diagnosis. Pediatr Radiol 37:1101–1109
11. Vicente J, Fuster-Garcia E, Tortajada S et al (2013) Accurate classification of childhood brain tumours by in vivo 1H MRS- a multicentre study. Eur J Cancer 49:658–667
12. Peet AC, Davies NP, Ridley L et al (2017) Magnetic resonance spectroscopy suggests key differences in the metastatic behavior of medulloblastoma. Eur J Cancer 43:1037–1044
13. Davies NP, Wilson M, Harris LM et al (2008) Identification and characterization of childhood cerebellar tumours by in vivo proton MRS. NMR Biomed 21:908–918
14. Scheneider JF, Confort-Gouny S, Viola A et al (2007) Multiparametric differentiation of posterior fossa tumors in children using diffusion-weighted imaging and short echo-time 1H-MR spectroscopy. J Magn Reson Imaging 26:1390–1398
15. Plaza MJ, Borja MJ, Altman N, Saigal G (2013) Conventional and advanced MRI features of pediatric intracranial tumors: posterior fossa and suprasellar tumors. AJR Am J Roentgenol 200:1115–1124
16. Panigrahy A, Krieger MD, Gonzalez-Gomez I et al (2006) Quantitative short echo time 1H-MR spectroscopy of untreated pediatric brain tumors: preoperative diagnosis and characterization. AJNR Am J Neuroradiol 27:560–572
17. Moreno-Torres A, Martínez-Pérez I, Baquero M et al (2004) Taurine detection by proton magnetic resonance spectroscopy in medulloblastoma: contribution to noninvasive differential diagnosis with cerebellar astrocytoma. Neurosurgery 55:824–829
18. Majós C, Alonso J, Aguilera C et al (2002) Adult primitive neuroectodermal tumor: proton MR spectroscopic findings with possible application for differential diagnosis. Radiology 225:556–566
19. Stefan D, Di Cesare F, Andrasescu A et al (2009) Quantification of magnetic resonance spectroscopy signals: the jMRUI software package. Meas Sci Technol 20:104–135

20. Tate AR, Underwood J, Acosta DM et al (2006) Development of a decision support system for diagnosis and grading of brain tumours using in vivo magnetic resonance single voxel spectra. NMR Biomed 19:411–434
21. Hochberg Y, Tamhane AC (1987) Multiple comparisons procedures. Wiley, New York
22. Lehman NL (2008) Central nervous system tumors with ependymal features: a broadened spectrum of primarily ependymal differentiation? J Neuropathol Exp Neurol 67:177–188
23. Ho VB, Smirniotopoulus JG, Murpphy FM, Rushing EJ (1992) Radiologic-pathologic correlation: haemangioblastoma. AJNR Am J Neuroradiol 13:1343–1352
24. Remke M, Hielscher T, Northcott PA et al (2011) Adult medulloblastoma comprises three major molecular variants. J Clin Oncol 29:2717–2723
25. Bourgouin PM, Tampieri D, Grahovac SZ, Léger C, Del Carpio R, Melançon D (1992) CT and MR findings in adults with cerebellar medulloblastoma: comparison with findings in children. AJR Am J Roentgenol 159:609–612
26. Armington WG, Osborn AG, Cubberley DA et al (1985) Supratentorial ependymoma: CT appearance. Radiology 157: 367–372
27. Shih RY, Smirniotopoulus JG (2016) Posterior fossa tumors in adult patients. Neuroimaging Clin N Am 26:493–510
28. Miller BL, Chang L, Booth R et al (1996) In vivo 1H MRS choline: correlation with in vitro chemistry/histology. Life Sci 58:1929–1935
29. Verma A, Kumar I, Verma N, Aggarwal P, Ojha R (2016) Magnetic resonance spectroscopy-revisiting the biochemical and molecular milieu of brain tumors. BBA Clin 5:170–178
30. Hattingen E, Raab P, Franz K, Zanella FE, Lanfermann H, Ulrich P (2008) Myo-inositol: a marker of reactive astrogliosis in glial tumors? NMR Biomed 21:233–241
31. Candiota AP, Majós C, Julià-Sapé M et al (2011) Non-invasive grading of astrocytic tumours from the relative contents of myo-inositol and glycine measured in vivo MRS. JBR-BTR 94:319–329